CONSTRUCTAL MULTI-SCALE PIN FINS

T. Bello-Ochende[a], J. P. Meyer[a*], A. Bejan[b]

[a]Department of Mechanical and Aeronautical Engineering, University of Pretoria,

Pretoria, 0002, South Africa,

[b]Department of Mechanical Engineering and Materials Science, Duke University

Box 90300, Durham, NC 27708-0300, USA

Abstract

In this paper we use constructal theory to determine the configuration of two rows of pin fins so that the total heat transfer rate is maximized. The heat transfer across the fins is by laminar forced convection bathed by a free-stream that is uniform and isothermal. The optimization is subjected to fixed total volume of fin materials. The dimensions of the optimized configuration are the result of balancing conduction along the fins with convection transversal to the fin. The resulting flow structure has multiple scales that are distributed non-uniformly through the flow structure. Numerical results on the effect of Reynolds number and the thermal conductivity ratio on the optimal configuration are reported. The results predicted based on scale analysis are in good agreement with the numerical results. The results also show that the flow structure performs best when the fin diameters and heights are non-uniform.

Keywords: fins, constructal, multiscale design, optimized configuration, heat transfer augmentation, extended surfaces, heat transfer density

Nomenclature

D_1 diameter of the first fin

D_2 diameter of the second fin

h heat transfer coefficient

H_1 height of the first fin

*Corresponding author. Tel: +27 12 420 2590; Fax: +27 362 5124
E-mail address: Josua.Meyer@up.ac.za (J. P. Meyer)

H_2 height of the second fin

H_u virtual extension on the upper boundary condition

k thermal conductivity

L the swept axial length

n normal

P pressure

Pr Prandtl number

q total heat transfer rate

$\tilde{q}$ dimensionless heat transfer density, Eq. (13)

Re_L Reynolds number ($U_\infty L/\nu$)

S_1 spacing between the first cylinder and the trailing edge

S_2 spacing between the D_1 and D_2 cylinders

T temperature

T_w wall temperature

T_∞ free stream temperature

u, v, w velocity components

U_∞ free stream velocity

V total volume of the fins

x, y, z cartesian coordinates

Greek symbols

α thermal diffusivity

μ viscosity

ν kinematic viscosity

ρ density

Ω interface between solid and fluid

λ Langrage multiplier

Subscripts

1 leading row

2 trailing row

max maximum

opt optimum

s solid

w wall

Superscripts

(~) dimensionless variables, Eqs. (3 - 13)

1. Introduction

Recent advances in the computational power of microprocessors have led to a significant increase in power densities in electronic devices and appliances. Under the conditions of high clock speeds and shrinking package size, the heat discharge per unit volume from these devices has increased dramatically over the past decade. As the power dissipation increases with shrinking package size, the density of the heat that is being discharged increases and the effective cooling technology becomes essential for reliable operation of electronic components. Therefore, various types of cooling systems and techniques [1-10] have been proposed and developed. One of the most recent techniques is constructal design [1, 2] which is now a growing field in thermal sciences. It is used as a method of discovering effective flow configurations for thermal and fluid systems. This

method is guided by the Constructal law: the progress made with this law to predict design in nature has been documented in the physics and biology literature. Reviews of this literature are provided by Refs. [11, 12].

In this paper we show that by using the constructal design method it is possible to optimize the electronic configuration to give maximum heat transfer subject to fixed volume and weight. The maximization of heat transfer rate subject to constant fin volume has attracted considerable attention. Schmidt [8] agued intuitively that there exists not only an optimum fin size when the profile shape is specified, but also an optimum profile shape that maximizes the total heat transfer rate. The optimum shape must be such that the temperature varies linearly along the fin. The optimum profile shape of fins with temperature-dependent conductivity was determined by Jany and Bejan [9], who showed that the fin shaped optimization has an important analog in the design of a long duct with fluid flow. The optimum dimension for a plate fin with fixed volume with a transversal laminar boundary layer was determined by Bejan [10].

Bejan [13] showed that the optimum fin shapes and dimensions can be determined based on purely thermodynamic grounds. They determined the optimal pin fin diameter and length for which the thermodynamic irreversibility (entropy generation rate) of the fin-fluid arrangement is a minimum. During this optimization procedure, the heat transfer through the base was kept constant. Recently Yang and Peng [14] conducted a numerical study of a pin-fin heat sink with non-uniform fin height, and concluded that the junction temperature can be reduced by increasing the pin height near the center of the heat sink. Furthermore the potential exists for optimizing the non-uniform fin height design. In recent years we are seeing an increase in the use of multi-objective algorithms [15-17] to solve optimization problems of extended surfaces for maximizing heat transfer and minimizing the hydraulic resistance.

The objective of this paper is to determine the optimal configuration of rows of pin fins that will maximizes the total heat transfer from the fins and the hot surfaces, subject to the constraints of fixed total volume and fixed volume of fin material. The pin-fin is bathed by a stream of fluid flowing over it. This work is based on balancing the transversal convective resistance and the conductive resistance along the fins. From this balance emerges the constructal configuration: rows of fins that have non-uniform dimensions, and are different than the convectional pin fins.

2. Model

Consider the two rows of a multi-scale cylindrical pin fin assembly as shown in Fig. 1. The distance between the first row of fins and the leading edge is S_1. The distance between the two rows is S_2. The fin heights are H_1 and H_2, while their respective diameters are D_1 and D_2. The swept length is L and it is fixed. The flow assembly is bathed by a free stream that is uniform and isothermal. Because of symmetry we select an elemental volume that contains only two fins on a rectangular wall base of swept length L and width $L/3$.

The objective is to discover the configuration (i. e. all the dimensions) such that the rate of heat transfer from the solid to the fluid is maximum subject to the constraint that the total volume of fin volume (V) is fixed

$$D_1^2 H_1 + D_2^2 H_2 = \frac{4}{\pi} V, \text{ constant} \tag{1}$$

This constraint is dictated by the weight and the material cost of the fins structure, which is a limiting parameter in the design of electronic devices and modern vehicles (e. g. aircraft, fuel efficient vehicles). In addition, there is the overall size constraint

$$S_1 + D_1 + S_2 + D_2 = L \tag{2}$$

The configuration has six dimensions that can vary (S_1, S_2, H_1, H_2, D_1, and D_2). We fix S_1 such that the first fin is close to the leading edge, and this leaves five dimensions in the design. Because of the two constraints (1, 2), the number of degrees of freedom is three. The

flow is assumed steady, laminar, incompressible and two-dimensional. All the thermo-physical properties are assumed constant. The conservation equations for mass, momentum and energy occupied by the fluid are

$$\frac{\partial \tilde{u}}{\partial \tilde{x}} + \frac{\partial \tilde{v}}{\partial \tilde{y}} + \frac{\partial \tilde{w}}{\partial \tilde{z}} = 0 \tag{3}$$

$$Re\left(\tilde{u}\,\frac{\partial \tilde{u}}{\partial \tilde{x}} + \tilde{v}\,\frac{\partial \tilde{u}}{\partial \tilde{y}} + \tilde{w}\frac{\partial \tilde{u}}{\partial \tilde{z}} \right) = -\frac{\partial \tilde{P}}{\partial \tilde{x}} + \nabla^2 \tilde{u} \tag{4}$$

$$Re\left(\tilde{u}\,\frac{\partial \tilde{v}}{\partial \tilde{x}} + \tilde{v}\,\frac{\partial \tilde{v}}{\partial \tilde{y}} + \tilde{w}\frac{\partial \tilde{v}}{\partial \tilde{z}} \right) = -\frac{\partial \tilde{P}}{\partial \tilde{y}} + \nabla^2 \tilde{v} \tag{5}$$

$$Re\left(\tilde{u}\,\frac{\partial \tilde{w}}{\partial \tilde{x}} + \tilde{v}\,\frac{\partial \tilde{w}}{\partial \tilde{y}} + \tilde{w}\frac{\partial \tilde{w}}{\partial \tilde{z}} \right) = -\frac{\partial \tilde{P}}{\partial \tilde{z}} + \nabla^2 \tilde{w} \tag{6}$$

$$RePr\left(\tilde{u}\,\frac{\partial \tilde{T}}{\partial \tilde{x}} + \tilde{v}\,\frac{\partial \tilde{T}}{\partial \tilde{y}} + \tilde{w}\frac{\partial \tilde{T}}{\partial \tilde{z}} \right) = \nabla^2 \tilde{T} \tag{7}$$

For the volume occupied by the cylindrincal fins, the energy equation reduces to

$$\nabla^2 \tilde{T} = 0 \tag{8}$$

where $\nabla^2 = \partial/\partial\tilde{x}^2 + \partial/\partial\tilde{y}^2 + \partial/\partial\tilde{z}^2$. The coordinate system ($\tilde{x}$, $\tilde{y}$, $\tilde{w}$) and velocity components ($\tilde{u}$, $\tilde{v}$, $\tilde{w}$) are defined in Fig. 1. Equations (4)-(7) are non-dimensionalized by defining variables

$$(\tilde{x},\ \tilde{y},\ \tilde{z}) = \frac{(x,\ y,\ z)}{L} \qquad (\tilde{u},\ \tilde{v},\ \tilde{w}) = \frac{(u,\ v,\ w)}{U_\infty} \tag{9}$$

$$\tilde{T} = \frac{T - T_\infty}{T_w - T_\infty} \qquad \tilde{P} = \frac{P}{\mu U_\infty / L} \tag{10}$$

where Pr is the Prandtl number ν/α, and Re is the Reynolds number

$$\mathrm{Re} = \frac{U_\infty L}{\nu} \tag{11}$$

The flow boundary conditions are: no slip and no penetration on the fins and the wall surfaces, and $\tilde{w} = 1$, $\partial\tilde{u}/\partial\tilde{z} = \partial\tilde{v}/\partial\tilde{z} = 0$ at the inlet of the flow assembly; $\partial(\tilde{u},\tilde{v},\tilde{w})/\partial\tilde{x} = 0$ at the exit and $\partial(\tilde{u},\tilde{v},\tilde{w})/\partial\tilde{y} = 0$, at the top of the computational domain and no flow and no penetration at the plane of symmetry. The thermal boundary conditions are: $\tilde{T} = 1$ on the wall surfaces, and $\tilde{T} = 0$ on the inlet plane of the computational domain. The planes of symmetry of the computational domain are adiabatic, that is $\left.\frac{\partial\tilde{T}}{\partial n}\right|_\Omega = 0$ on the plane of symmetry. The continuity of the temperature and flux at the interface of the solid and fluid surfaces requires

$$-\tilde{k}\left.\frac{\partial\tilde{T}_s}{\partial n}\right|_\Omega = -\left.\frac{\partial\tilde{T}}{\partial n}\right|_\Omega \tag{12}$$

where $\tilde{k}$ is the conductivity ratio k_s/k.

The spacing between the fins varies, and the shapes of the fins are allowed to morph. We are interested in the geometric configuration $(\tilde{D}_1, \tilde{D}_2, \tilde{H}_1, \tilde{H}_2, \tilde{S}_2)$ in which the overall heat transfer between the elemental $\tilde{T}_w$ and the fin surfaces and the surrounding flow is a maximum. The dimensionless measure of the overall heat transfer is

$$\tilde{q} = \frac{q/L}{k\ (T_w - T_\infty)} \tag{13}$$

where q is the total heat transfer rate integrated over the surface of the fins and the elemental surfaces. This $\tilde{q}$ formula is the dimensionless global thermal conductance of the volume element.

3. Numerical procedure

Equations (3)-(8) were solved by using a finite-volume computational fluid dynamics code [18]. The domain is discretized using polyhedral elements, and the governing equations are integrated on each control volume. Second order schemes are used for the diffusive terms. The pressure-velocity coupling is performed with the SIMPLE algorithm. Convergence is obtained when the normalized residuals for the mass and momentum equations are smaller than 10^{-4}, and the residual of the energy equation becomes smaller than 10^{-7}.

Virtual extensions have been added to the upper part of the numerical domain in order to account adequately for possible outflow through the upper boundary. The length of the virtual extensions zone was chosen long enough so that a doubling of the length resulted in variations of the total heat transfer rate [Eq. (13)] smaller than 1%. For example when Re = 10^2, Pr = 0.71 and D_2/D_1 = 1, we found out that the required extension is $\tilde{H}_u$ = 0.2. Grid independence tests were carried out for all the fin arrangements. The tests showed that for a control volume with a mesh size of 0.005 per unit length in the x -direction, 0.01 per unit length in the y-direction, and 0.01 per unit length in the z-direction assured a grid independent solution in which the maximum changes in total heat transfer rate are less than 1% when the mesh per unit length is doubled sequentially. To further ensure grid independence we refined the meshes in the vicinity of the optimal configurations so that the effect of grid size on the final numerical solution was essentially eliminated.

4. Optimization of multi-scale pin fins

The search for optimal flow and heat sink configurations was organized in three nested optimization loops. The fin flow structure has three degrees of freedom which are designated as $\frac{H_2}{H_1}, \tilde{S}_2$ and $\frac{D_2}{D_1}$. We started by fixing the distance between the first fin and the leading edge, $\tilde{S}_1 = 0.05$, with the total volume of the fins set at $\tilde{V} = 0.01$. The degrees of

freedom that remain are the ratios of the fins height, $\frac{H_2}{H_1}$, and the diameters ratio $\frac{D_2}{D_1}$, and the spacing between the cylinders, $\tilde{S}_2$. The dimensions of the flow structure are set as follows: the non-dimensionalized flow length $\tilde{L}$ is set equal to 1, the flow width (the distance between two symmetry planes, in the *x*-direction) is $\tilde{L}/3$, c.f. Fig. 1, and the virtual extension was fixed at $\tilde{H}_u = 0.2$. For the first run of our numerical procedure we fixed the Reynolds number at 50, the non-dimensionless thermal conductivity ratio $\tilde{k}$ at 100, and the diameter ratio $\frac{D_2}{D_1}$ at 1. The distance between the two pin fins $\tilde{S}_2$ was set equal to 0.1, and then the fin height ratio was varied. An optimal height ratio was found for this configuration. This procedure was repeated for other $\tilde{S}_2$ values in the range $0.05 \le \tilde{S}_2 \le 0.2$, as shown in Fig. 2, until an overall optimum was found for this configuration, i. e. the optimal height ratio $\frac{H_2}{H_1}$ that corresponds with the maximum total heat transfer rate.

The diameter ratio $\frac{D_2}{D_1}$ was then increased to 1.1 and the procedure was performed in the range $0.05 \le \tilde{S}_2 \le 0.2$, as shown in Fig. 3. A new optimal configuration was found with a corresponding maximum total heat transfer rate. Figure 4 shows the behavior of the optimal configuration for $\frac{D_2}{D_1}$ = 1.2. Figures 2-4 show that as the $\frac{D_2}{D_1}$ increases the optimal $\frac{H_2}{H_1}$ decreases. The optimal pin-fin configuration for *Re* = 50, and $\tilde{k}$ = 100 lies in the design domain $0.05 \le \tilde{S}_2 \le 0.2$, $1 \le \frac{D_2}{D_1} \le 1.2$., and $0.9 \le \frac{H_2}{H_1} \le 1.2$.

Figure 5 summarizes the optimal designs, and shows the effect of the diameter ratio on the maximum total heat transfer rate for the range of parameters given. The best $\frac{D_2}{D_1}$ value is approximately 1.1, but at this late stage of optimization the effect of $\frac{D_2}{D_1}$ is weak.

The optimization procedure was extended to higher Reynolds number, for example Re = 200 in Fig. 6. The influence of the Reynolds number on the optimal fin to fin distance $\tilde{S}_{2,opt}$ is insignificant over the Re range considered. Similarly, the optimal height ratio, $\left(\frac{H_2}{H_1}\right)_{opt}$ is robust, as the effect of Reynolds number on this parameter is fairly insignificant. In this range of Reynolds numbers $\left(\frac{H_2}{H_1}\right)_{\text{opt}}$ is equal to 0.9. It indicates that the height of the second row of fins should be slightly lower than that of the first rows. Figure 6 also shows that $\left(\frac{D_2}{D_1}\right)_{\text{opt}}$ increases with Re. This is an important result, as this establishes that the diameters of the fins must not be uniform. The results of Fig. 6 were correlated within an error of less than one percent by

$$\left(\frac{D_2}{D_1}\right)_{opt} = 0.62\, Re^{0.146} \tag{14}$$

The maximum total heat transfer rate increases with the Reynolds number, and from Fig. 6 this trend was correlated with an error of less than one percent by

$$\tilde{q}_{\max} = 2.16\, Re^{0.32} \tag{15}$$

5. Effect of dimensionless conductivity ratio

The effect of the thermal conductivity ratio $\tilde{k}$ was also investigated. In Fig. 7 the results are reported for the range $30 \leq \tilde{k} \leq 300$ at a Reynolds number of 100. The figure shows that the optimal height ratio is fairly constant for the $\tilde{k}$ range considered. The relationship between the dimensionless thermal conductivity and the optimal diameter ratio shows that as $\tilde{k}$ increases the optimal diameter ratio decreases. This relationship is correlated by

$$\left(\frac{D_2}{D_1}\right)_{opt} = 2.54\,\tilde{k}^{-0.16} \tag{16}$$

The optimal spacing between the pin fins shows that as $\tilde{k}$ increases the optimal spacing $\tilde{S}_{2,opt}$ also increases. The effect of $\tilde{k}$ on the maximum total heat transfer rate shows a similar trend as with respect to the Reynolds number. From Fig. 7 this can be correlated with an error of less than one percent by the relation

$$\tilde{q}_{\max} = 2.48\,\tilde{k}^{0.29} \tag{17}$$

Figure 8 shows the temperature distribution in the centre plane of the pin-fin assembly, for different Reynolds numbers and different dimensionless thermal conductivity ratios. All the temperature profiles are presented for Pr = 0.71. The temperature ranges between two colors, red ($\tilde{T}=1$) and blue ($\tilde{T}=0$). The temperature profiles and the fin configurations change with the Reynolds number. As *Re* increases the fin heights decrease and the fins diameters increase. Similarly, as *Re* increases the blue color of the temperatures profiles penetrates the fin structure, and this can be attributed to the increase in the flow strength and the flattening of the thermal boundary layers.

The effect of the thermal conductivity ratio is displayed in Fig. 9. As the dimensionless thermal conductivity ratio increases, the fin height increases and results in the decrease in the diameters of the pin-fins.

6. Scale analysis

The scaling trends discovered numerically in the preceding sections can be explained on the basis of scale analysis. First, each fin achieves its highest thermal conductance at fixed volume (or minimal volume at fixed conductance) when its entire volume is active in transferring heat. This happens when the distance of heat conduction penetration along the fins matches the lateral length engaged in convective heat transfer,

$$k_s D_1^2 \frac{\Delta T_1}{H_1} \sim h_1 D_1 H_1 \Delta T_1 \tag{18}$$

$$k_s D_2^2 \frac{\Delta T_2}{H_2} \sim h_2 D_2 H_2 \Delta T_2 \tag{19}$$

These equations yield

$$\frac{D_1}{H_1^2} \sim \frac{h_1}{k_s}, \qquad \frac{D_2}{H_2^2} \sim \frac{h_2}{k_s} \tag{20, 21}$$

The heat transfer coefficients (h_1, h_2) depend on the fin diameters (D_1, D_2) and the free stream velocity (U_∞), which is the same for both fins. If we assume that D_1 is not much different than D_2, then we approximate h_1 as being nearly the same as h_2,

$$h_1 = h_2 = h \tag{22}$$

After combining Eqs. (18) – (22), the total heat transfer rate vehicled by the two fins is

$$q \sim \frac{h^2}{k_s}(H_1^3 \Delta T_1 + H_2^3 \Delta T_2) \tag{23}$$

Here we make a distinction between the temperature difference spanned by the first fin, $\Delta T_1 = T_w - T_\infty$, and the temperature difference spanned by the second fin, $\Delta T_1 = T_w - T_i$. The intermediate temperature T_i falls between T_w and T_∞ because the second fin is in the thermal wake of the first. In other words, the first fin warms up the free stream that bathes the second fin. In sum, ΔT_1 and ΔT_2 are of the same order but

$$\Delta T_1 \geq \Delta T_2 \tag{24}$$

The objective is to maximize the q expression (23) subject to the total fin volume constraints (1), which in view of Eqs. (20, 21) becomes

$$V \sim \left(\frac{h}{k_s}\right)^2 (H_1^5 + H_2^5), \text{ constant} \tag{25}$$

Based on the method of Lagrange multipliers, the maximization of the expression (23) subject to the volume constraints (25) yields

$$\frac{H_1}{H_2} = \left(\frac{\Delta T_1}{\Delta T_2}\right)^{1/2} \tag{26}$$

In view of Eq. (24), the conclusion is that $H_1 \geq H_2$, which agrees with the results displayed in Figs. 6 and 7. An additional implication of this scale analysis is with respect to anticipating the ratio $\frac{D_2}{D_1}$, which according to the scaling rules (20, 21) should be

$$\frac{D_1}{D_2} \sim \left(\frac{H_1}{H_2}\right)^2 \tag{27}$$

In view of Eq. (26), the ratio of diameters should be

$$\frac{D_1}{D_2} \sim \frac{\Delta T_1}{\Delta T_2} \geq 1 \tag{28}$$

This conclusion agrees in an order of magnitude sense with the data plotted in Figs. 6 and 7.

The ratio $\frac{D_1}{D_2}$ becomes smaller than 1 when $\tilde{k}$ increases (Figs 7) and when Re decreases (Fig. 6).

7. Conclusions

In this paper we described the procedure for the conceptual design of a new generation of multi-scale pin arranged in a row using the principles of constructal theory. The pin-fins are cooled by laminar forced convection. The total fin volume of the pins was fixed. Numerical optimization was performed to determine the optimal configuration (relative diameters, heights and spacings between fins). The optimized configuration is the result of balancing conduction along the fins with convection transversal to the fins. The resulting flow structure has multiple scales that are distributed non-uniformly throughout the flow structure.

The results predicted by using scale analysis are in agreement with the numerical results, however, future work may consider the more general situation in which the assumption $h_1 \simeq h_2$ [Eq. (22)] is not made. In conclusion, the pin-fins flow structure performs best when the pin-fin diameters and heights are non-uniform. Future work may also consider the optimization of arrays of multiscale fins with more than two rows.

Acknowledgements

Tunde Bello-Ochende acknowledges the support from the University of Pretoria, Research Development Programme (RDP) and the National Research Foundation (NRF) of South Africa, NACoE, TESP. EEDSM and the SANERI/UP/US collaboration. Adrian Bejan's research was supported by a grant from the National Science Foundation.

References

[1] A. Bejan, S. Lorente, Design with Constructal Theory, Hoboken, 2008.

[2] A. Bejan, Heat Transfer, Wiley, New York, 1993.

[3] T. Bello-Ochende, A. Bejan, Maximal heat transfer density: Plates with multiple lengths in forced convection, Int. J. of Thermal Sciences, 43 (2004) 1181-1186.

[4] S. J. Kim, S. W. Lee, eds., Air Cooling Technology for Electronic Equipment, CRC Press, Boca Raton, FL, 1996, Chapter 1.

[5] R. S. Matos, T. A. Laursen, J. V. C. Vargas, A. Bejan, Three-dimensional optimization of staggard finned circular and elliptic tubes in forced convection, Int. J. Thermal Sciences 43 (2004) 447 – 487.

[6] F. Bobaru, S. Rachakonda, Optimal shape profiles for cooling fins of high and low conductivity, Int. J. Heat Mass Transfer 47 (23) (2004) 4953-4966.

[7] A. K. da Silva, L. Gosselin, On the thermal performance of an internally finned three-dimensional cubic enclosure in natural convection, Int. J. Therm. Sci. 44 (6) (2005) 540- 546.

[8] E. Schmidt, Die Wärmeübertragung durch Rippen, Z. Ver. Dt. Ing., 70 (1926) 885-889, 947-951.

[9] P. Jany, A. Bejan, Ernst Schmidt' approach to fin optimization: an extension to fins with variable conductivity and the design of ducts for fluid, Int. J. Heat Mass Transfer, 37 (1998) 1635 – 1644.

[10] A. Bejan, Convective Heat Transfer, third edition, Wiley, New York, 2004.

[11] A. H. Reis, Constructal Theory: from engineering to physics, and how flow systems develop shape and structure, Appl. Mech. Review 59 (2006) 269 -282.

[12] A. Bejan and S. Lorente, Constructal theory of generation of configuration in nature and engineering, J. Appl. Phys., 100 (2006) 041301.

[13] A. Bejan, Entropy Generation through Heat and Fluid Flow, Wiley, New York, 1982.

[14] Y.-T.Yang, H.- S. Peng, Numerical study of pin-fin heat with un-uniform fin height design, Int. J Heat Mass Transfer, 51 (2008) 4788-4796.

[15] G. Fabbri, A genetic algorithm for fin profile optimization, Int. J. Heat Mass Transfer 40 (9) (1997) 2165-2172.

[16] K. Foli, T. Okabe, M. Olhofer, Y. Jin, B. Sendhoff, Optimization of micro heat exchanger: CFD, analytical approach and multi-objective evolutionary algorithms, Int. J. Heat Mass Transfer 49 (2006) 1090-1099.

[17] D. Copiello, G. Fabbri, Multi-objective genetic optimization of the heat transfer from longitudinal wavy fins, Int. J. Heat Mass Transfer, 52 (2009) 1167-1176.

[18] www.fluent.com.

List of Figures

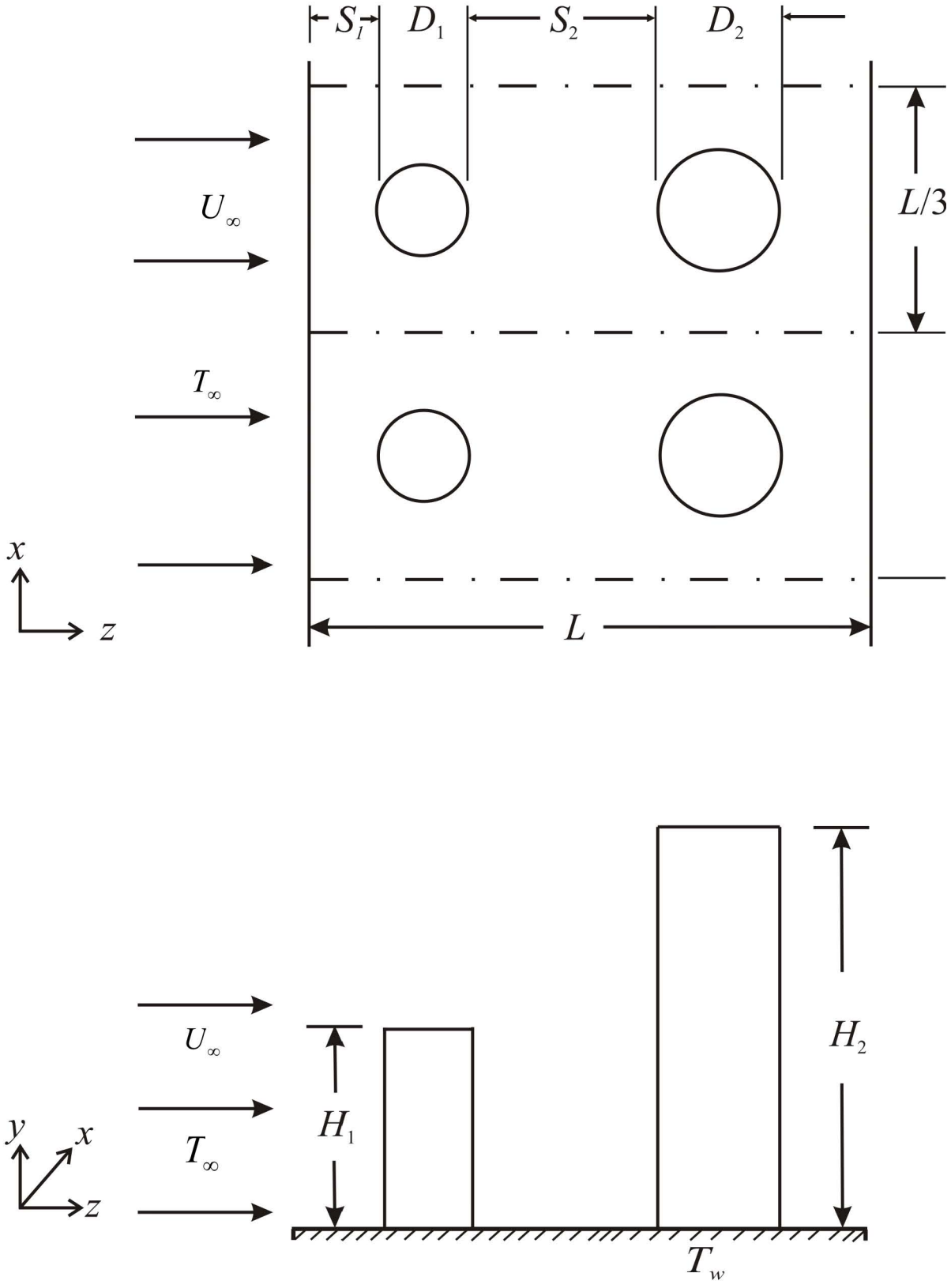

Figure 1

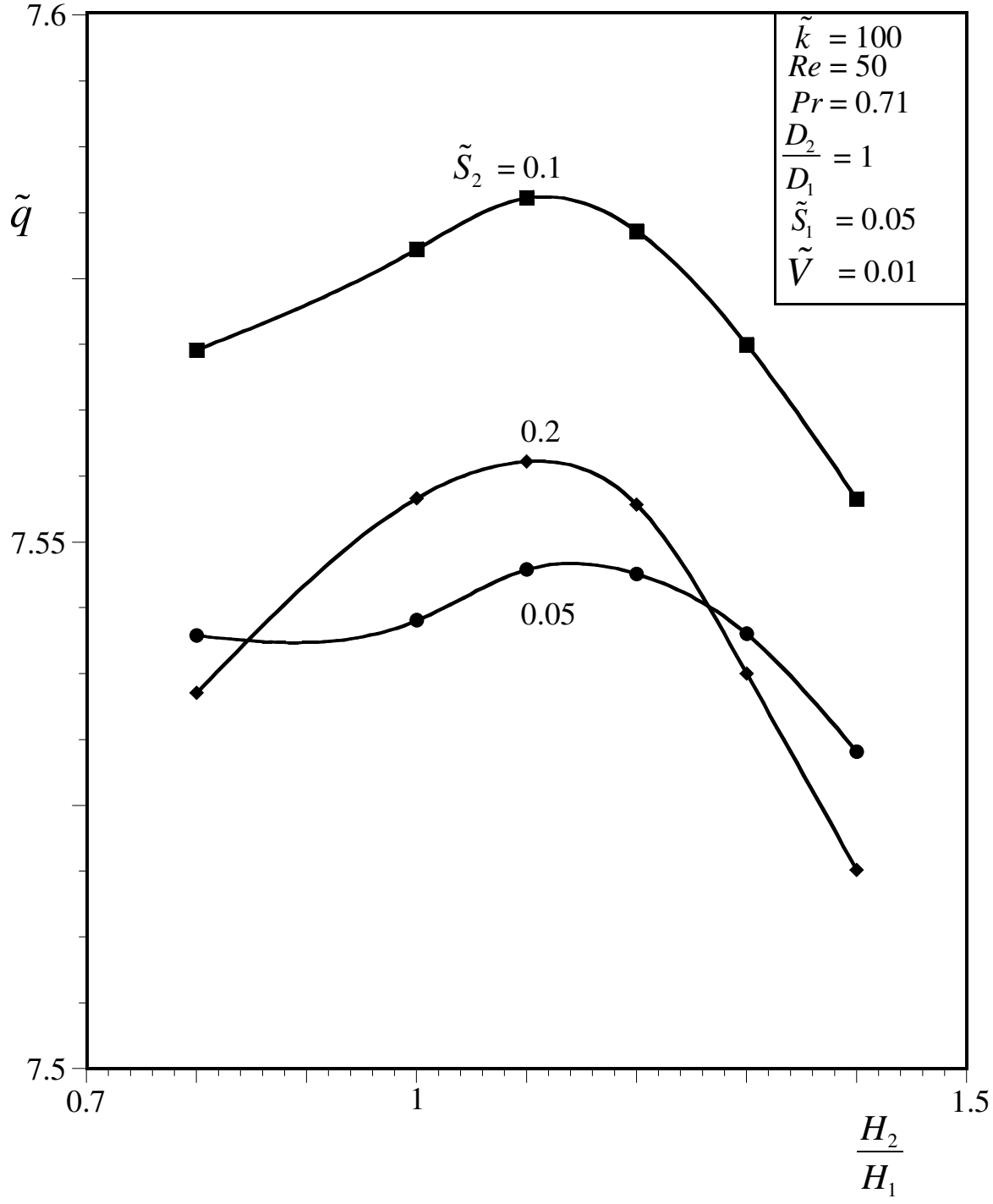
7.6
7.55
7.5
$\tilde{q}$
$\tilde{k}$ = 100
Re = 50
Pr = 0.71
$\frac{D_2}{D_1}$ = 1
$\tilde{S}_1$ = 0.05
$\tilde{V}$ = 0.01
$\tilde{S}_2$ = 0.1
0.2
0.05
0.7
1
1.5
$\frac{H_2}{H_1}$

Figure 2

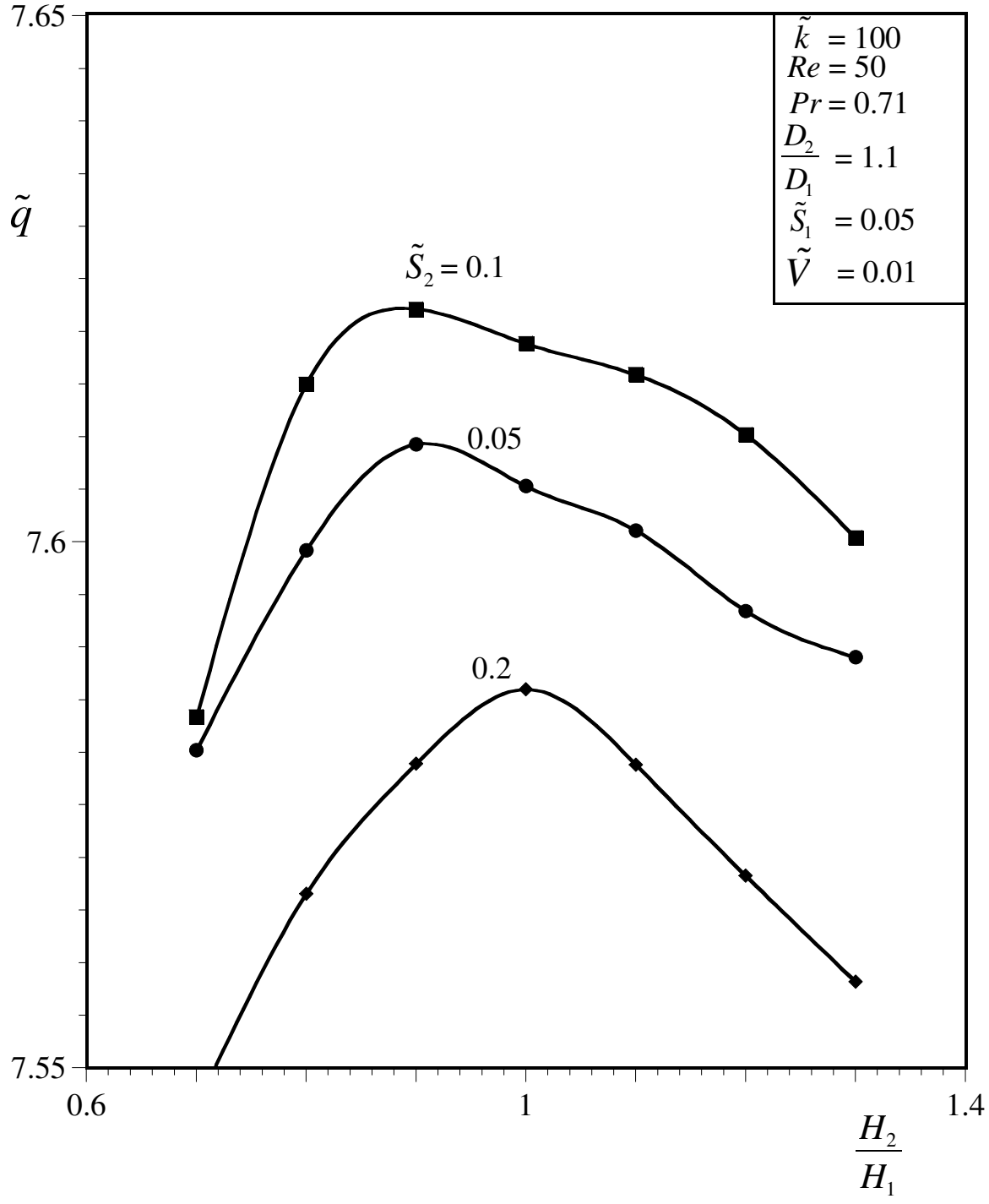
7.65
7.6
7.55
$\tilde{q}$
$\tilde{k} = 100$
$Re = 50$
$Pr = 0.71$
$\frac{D_2}{D_1} = 1.1$
$\tilde{S}_1 = 0.05$
$\tilde{V} = 0.01$
$\tilde{S}_2 = 0.1$
0.05
0.2
0.6
1
1.4
$\frac{H_2}{H_1}$

Figure 3

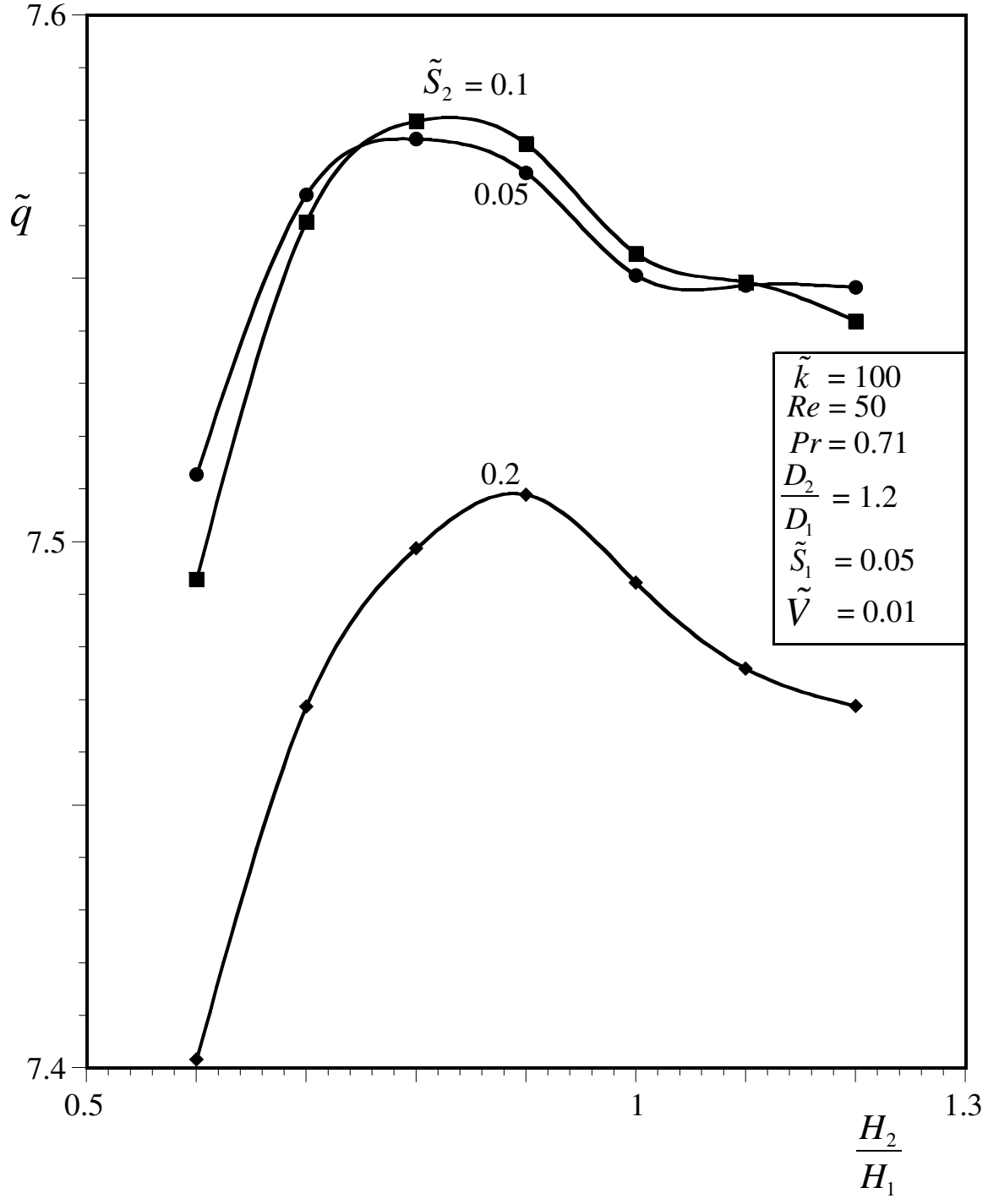
7.6
7.5
7.4
$\tilde{q}$
$\tilde{S}_2 = 0.1$
0.05
0.2
$\tilde{k} = 100$
$Re = 50$
$Pr = 0.71$
$\frac{D_2}{D_1} = 1.2$
$\tilde{S}_1 = 0.05$
$\tilde{V} = 0.01$
0.5
1
1.3
$\frac{H_2}{H_1}$

Figure 4

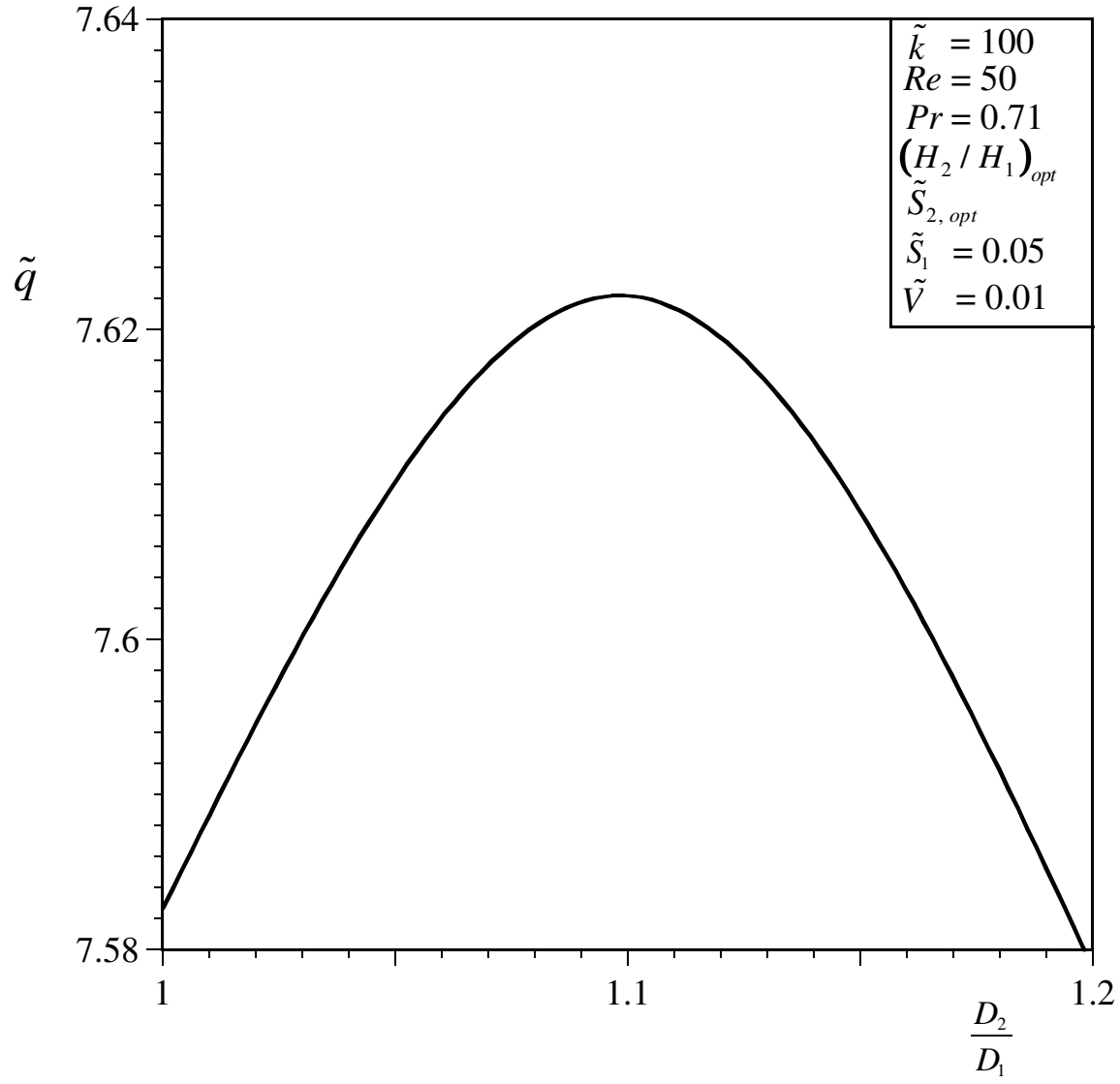
7.64
7.62
7.6
7.58
$\tilde{q}$
1
1.1
1.2
$\frac{D_2}{D_1}$
$\tilde{k}$ = 100
Re = 50
Pr = 0.71
$(H_2 / H_1)_{opt}$
$\tilde{S}_{2,\,opt}$
$\tilde{S}_1$ = 0.05
$\tilde{V}$ = 0.01

Figure 5

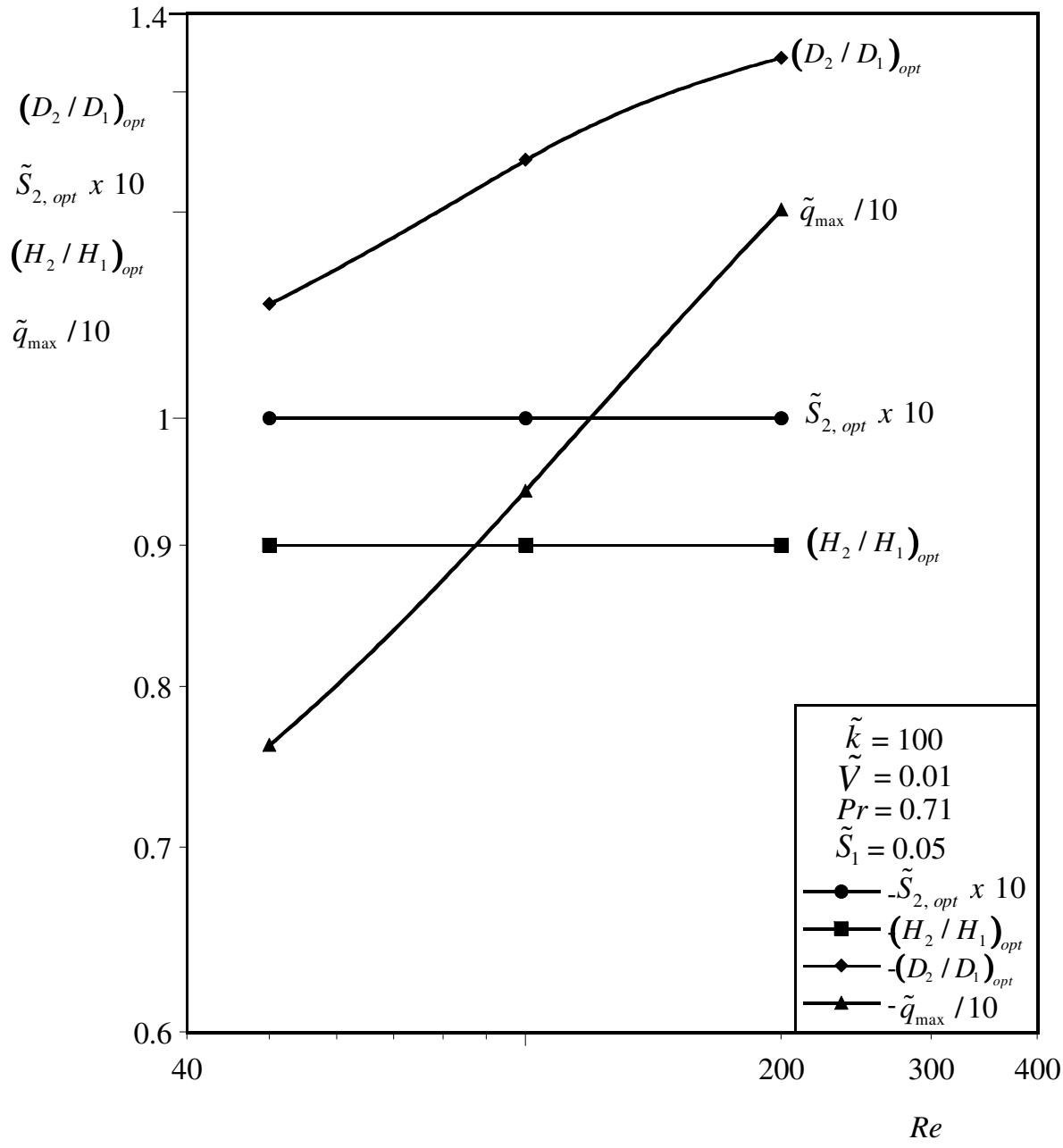
1.4
1
0.9
0.8
0.7
0.6
40
200
300
400
Re
$(D_2 / D_1)_{opt}$
$\tilde{S}_{2,\,opt}$ x 10
$(H_2 / H_1)_{opt}$
$\tilde{q}_{\max}$ /10
$\tilde{k}$ = 100
$\tilde{V}$ = 0.01
Pr = 0.71
$\tilde{S}_1$ = 0.05

Figure 6

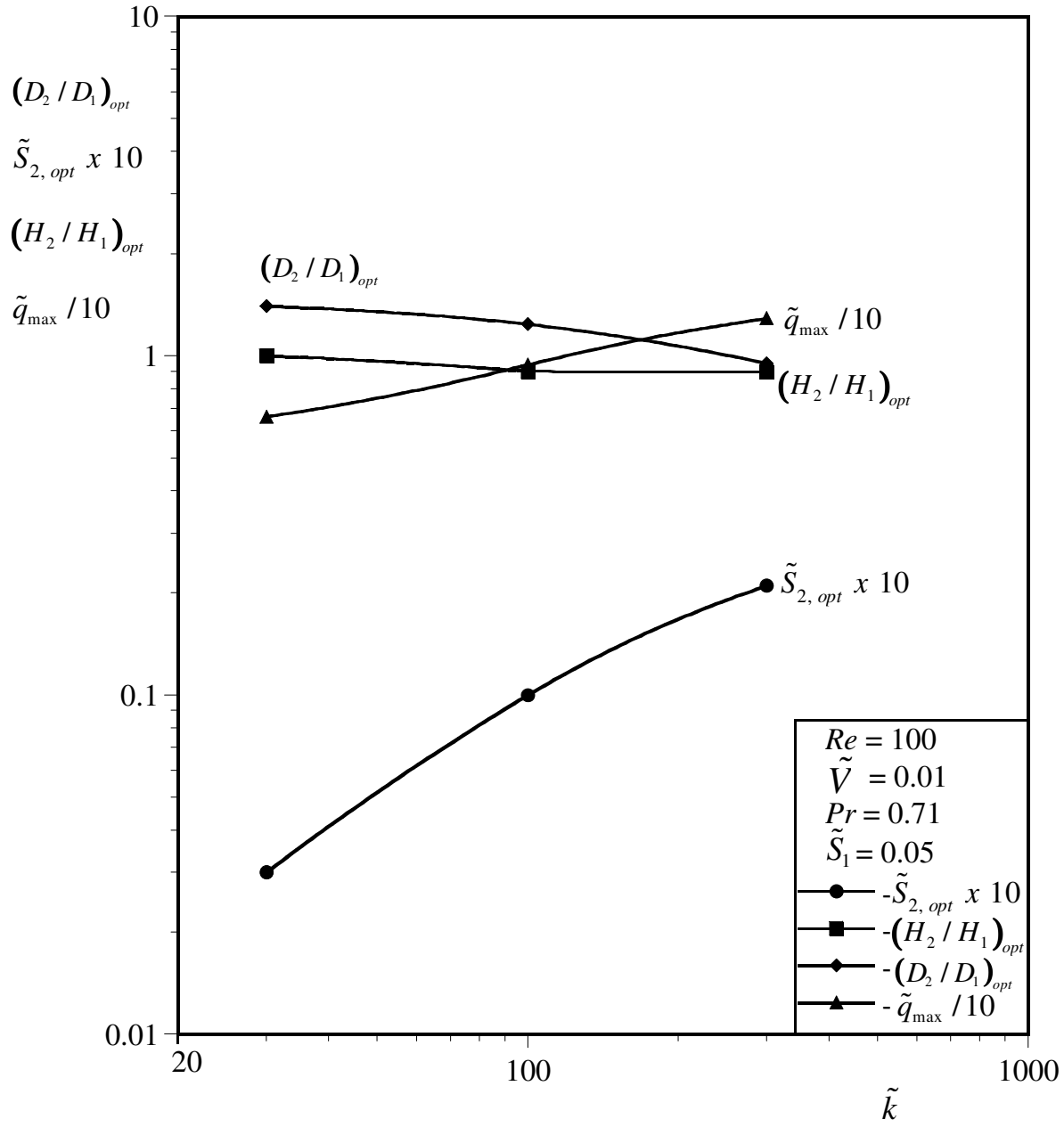
10
1
0.1
0.01
$(D_2 / D_1)_{opt}$
$\tilde{S}_{2,\,opt}\ x\ 10$
$(H_2 / H_1)_{opt}$
$\tilde{q}_{\max}\ /10$
$(D_2 / D_1)_{opt}$
$\tilde{q}_{\max}\ /10$
$(H_2 / H_1)_{opt}$
$\tilde{S}_{2,\,opt}\ x\ 10$
$Re = 100$
$\tilde{V} = 0.01$
$Pr = 0.71$
$\tilde{S}_1 = 0.05$
$-\tilde{S}_{2,\,opt}\ x\ 10$
$-(H_2 / H_1)_{opt}$
$-(D_2 / D_1)_{opt}$
$-\tilde{q}_{\max}\ /10$
20
100
1000
$\tilde{k}$

Figure 7

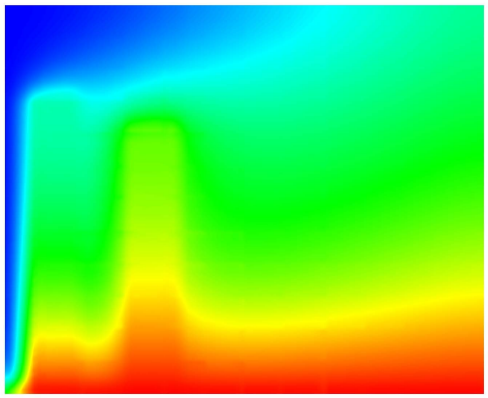

(a)

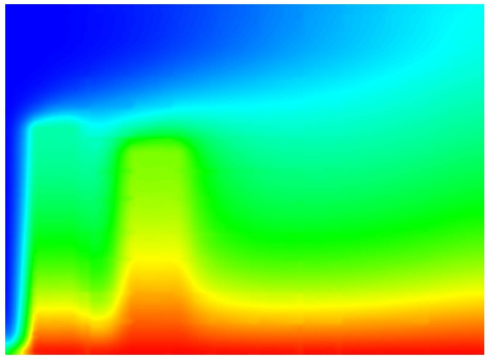

(b)

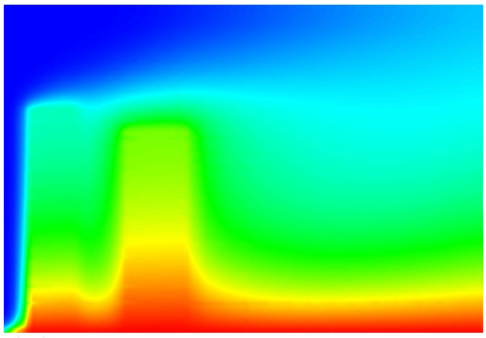

(c)

Figure 8

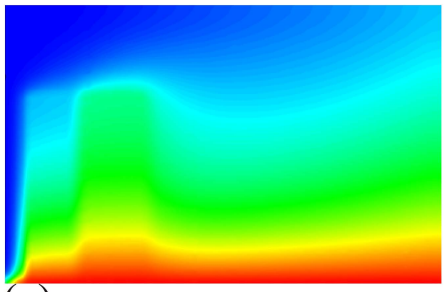

(a)

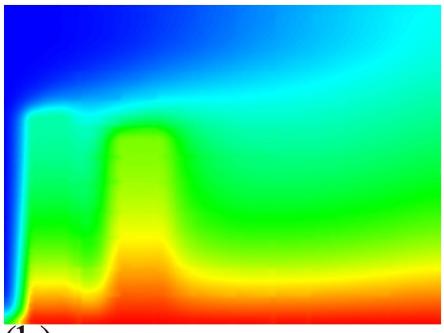

(b)

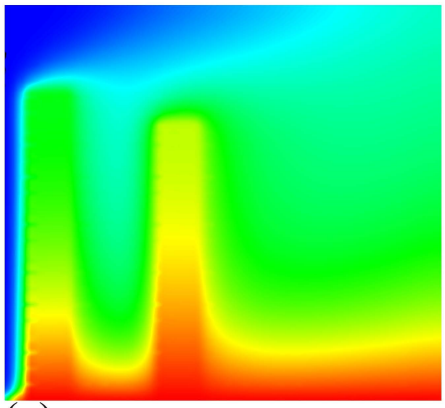

(c)

Figure 9